ACKNOWLEDGMENT

The authors are grateful to Prof. H. L. Hartnagel for his continuous support and encouragement.

REFERENCES

[1] J. Meixner, "The behavior of electromagnetic fields at edges," *IEEE Trans. Antennas Propagat.*, vol. AP-20, pp. 442–446, July 1972.
[2] R. Mittra and S. W. Lee, *Analytical Techniques in the Theory of Guided Waves*. New York: Macmillan, 1971, sec. 1.3.
[3] A. S. Omar and K. F. Schünemann, "Application of the generalized spectral-domain technique to the analysis of rectangular waveguides with rectangular and circular inserts," *IEEE Trans. Microwave Theory Tech.*, vol. 39, pp. 944–952, June 1991.
[4] W. Heinrich, "Full-wave analysis of conductor losses on MMIC transmission-lines," *IEEE Trans. Microwave Theory Tech.*, vol. 38, pp. 1468–1472, Oct. 1990.
[5] S. T. Peng, C. K. C. Tzuang, and Chu-Dong Chen, "Full-wave analysis of lossy transmission line incorporating the metal modes," *1990 IEEE MTT-S Int. Microwave Symp. Dig.*, Dallas, TX, vol. 1, pp. 171–174.
[6] R. Faraji-Dana and Y. L. Chow, "The current distribution and a.c. resistance of a microstrip structure," *IEEE Trans. Microwave Theory Tech.*, vol. 38, pp. 1268–1277, Sept. 1990.
[7] F. J. Schmückle and R. Pregla, "The method of lines for the analysis of lossy planar waveguides," *IEEE Trans. Microwave Theory Tech.*, vol. 38, pp. 1473–1479, Oct. 1990.
[8] W. Schröder and I. Wolff, "Full-wave analysis of normal- and superconducting transmission lines by hybrid-mode boundary integral equation method," in *1991 IEEE MTT-S Int. Microwave Symp. Dig.*, Boston, MA, vol. 1, pp. 341–344.
[9] R. Faraji-Dana and Y. Chow, "Edge condition of the field and ac resistance of a rectangular strip conductor," *IEEE Proc*, vol. 137, pt. H, pp. 133–140, Apr. 1990.
[10] W. Heinrich, "Conductor losses and their influence on circuit performance in planar MMIC's," in *Proc. Workshop F, 1991 MTT-S IEEE Int. Microwave Symposium*, Boston, MA.

Experimental Wide-Stopband Filters Utilizing Asymmetric Ferrite Junctions

H. How, Y. Liu, S. Zhang, C. Vittoria, C. Carosella, and V. Folen

***Abstract*—Filters incorporating asymmetric stripline Y-junction circulators have been fabricated and tested over the frequency range of 0.05 to 18 GHz. The passband frequency was near 2 GHz. The insertion loss was ~2 dB and the stopband extended from 4.5 to 18 GHz with transmission ≤ −30 dB. The filter includes ferrite discs in which high order modes have been eliminated as calculated in an earlier paper [2].**

INTRODUCTION

Filter designs incorporating ferrite materials have been developed for the past 25 years. Typically a polished sphere of single crystal YIG is fed through two orthogonal semi-circular wire loops such that the two wires become tightly coupled at the ferrimagnetic resonant frequency of the YIG sphere [1]. However, this design is susceptible to magnetostatic mode excitations above and below the main ferrimagnetic resonance mode. In addition, instabilities of the spin waves can induce the excitation of other subsidiary resonance modes. Altogether, excitations of these extraneous modes give rise to spurious transmissions at frequencies off the fundamental passband frequency. The power handling capacity in a resonant device is therefore quite low (~100 mW). In a previous paper [2] we investigated the feasibility of constructing a ferrite filter utilizing a Y-junction circulator design. By careful design of the junction geometry high order modes of excitations can be effectively suppressed and, hence, the stopband transmission of the device can be extended many times the fundamental frequency. Since wide stopband filters are currently needed for radome applications, we find here an example of ferrite devices that can be utilized to protect electronic components in high-power and/or high-noise environments. For a typical stripline circulator operating below 30 GHz the CW power handling capability can be as high as several hundred watts [3], since non-resonant properties of the ferrite are utilized in the microwave transmission mechanism.

A circulator is defined as a three-port device arranged such that the energy entering a port is coupled to an adjacent port but not to the third port. A circulator requires its three ports to be arranged symmetrically with respect to one another. However, one may relax this 3-fold symmetry to obtain one more degree of freedom in designing a circulator filter. Strictly speaking, this asymmetric design cannot be referred to as a circulator design and, therefore, we call our device a circulator design only under a restricted basis. In [2] we have established the circulation conditions for an asymmetric circulator, which determined in turn the radius of the ferrite disc and the dielectric ratio of the ferrite and the dielectric filling material [2].

In this paper we report our experimental work following the design conditions predicted by the theory [2]. We have fabricated several asymmetric circulators using three different kinds of ferrite materials. Experimentally, we find that transmissions due to high order mode excitations have been effectively suppressed and the reflection and transmission characteristics compare reasonably well with our calculations [2]. Using two circulators in cascade we measure 2.1 dB insertion loss, 33 dB isolation, and the stopband extending more than two octaves of the transmission frequency.

EXPERIMENTS

Fig. 1 depicts the geometry of an asymmetric circulator where the three ports are designated as the input, output, and isolated ports. The angle θ denotes half the asymmetric port separation angle (not necessarily equal to 60°), and ψ is half the suspension angle of the three ports. As predicted in [2] a circulator filter design can be realized by assigning the two angles θ and ψ both equal to 45°. Furthermore, the theory also predicts the following values:

$$\omega_o/\omega_m = 2.1, \quad \omega_f/\omega_m = 2.0, \quad \gamma\Delta H/\omega_m = 0.012,$$
$$\mu = 6.12, \quad \kappa = 4.88, \quad \mu_{\text{eff}} = 2.23,$$
$$\epsilon_d/\epsilon_f = 0.092, \quad x = 0.157, \quad z = 4.92,$$

where μ and κ are the Polder tensor elements defined by

$$\mu = 1 + \frac{\omega_m\omega_o}{\omega_o^2 - \omega^2}, \quad \kappa = \frac{\omega_m\omega}{\omega_o^2 - \omega^2},$$

Manuscript received January 25, 1991, revised July 18, 1991. This work was supported by ONR and the Naval Research Laboratory.

H. How, Y. Liu, S. Zhang, and C. Vittoria are with the Electrical and Computer Engineering Department, Northeastern University, Boston, MA 02115.

C. Carosella and V. Folen are with the Naval Research Laboratory, Washington, DC 20375.

IEEE Log Number 9103903.

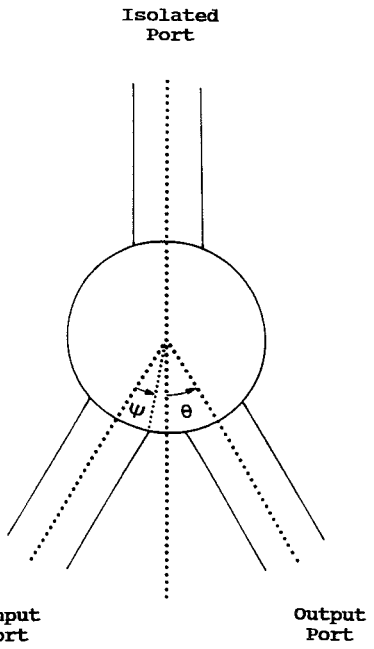

Fig. 1. Geometry of an asymmetric circulator.

and ω_m and ω_o are given by

$$\omega_m = 4\pi\gamma M_s, \quad \omega_o = \gamma H_i.$$

Here γ is the gyromagnetic ratio, $4\pi M_s$ the saturation magnetization, ω_f the circulation frequency, ΔH the linewidth, H_i the dc internal field, and ϵ_f and ϵ_d are the dielectric constants for the ferrite and the dielectric filling material, respectively. The effective permeability of the ferrite is

$$\mu_{\text{eff}} = \frac{\mu^2 - \kappa^2}{\mu},$$

the wave propagation constant and the intrinsic wave impedance of the ferrite are, respectively,

$$k = \frac{\omega}{c}\sqrt{\epsilon_f \mu_{\text{eff}}}, \quad Z_{\text{eff}} = \sqrt{\frac{\mu_o \mu_{\text{eff}}}{\epsilon_o \epsilon_f}}$$

with μ_o, ϵ_o, and c being the permeability, permittivity, and the speed of light in vacuum, respectively. The two parameters x and z are defined as

$$x = kR, \quad z = Z_{\text{eff}}/Z_{\text{in}},$$

and R and Z_{in} denote the radius of the ferrite disc and the input impedance of the device. When x and z values are used, the theory requires R and Z_{in} to be expressed as

$$R = \frac{563}{4\pi M_s \sqrt{\epsilon_f}}\,(\text{cm}), \quad Z_{\text{in}} = \frac{114}{\sqrt{\epsilon_f}}\,(\text{ohm}),$$

where $4\pi M_s$ is in unit of Gauss.

We chose three ferrite materials which were furnished by Trans-Tech, Inc. (Adamstown, MD). The ferrites were either magnesium ferrite (TT1-414) or nickel ferrites (TT2-113 and TT2-130). Table I lists the magnetic and physical design parameters of the ferrite discs. In Table I h denotes the height of the disc, D (= 2R) the diameter of the disc, and N_z the axial demagnetizing factor as calculated from [4]

$$N_z = (1 + e^2)(e - \tan^{-1} e)/e^3.$$

The ferrite disc is approximated as an oblate spheroid with eccentricity

$$e \approx \sqrt{D^2 - h^2}/h.$$

The dc internal field is therefore

$$H_i = H_o - 4\pi M_s N_z,$$

where H_o is the external applied field. Experimentally, we used neodymium permanent magnet discs to bias the ferrites to a maximum biasing field of 4000 Oe. The permanent magnets are designed to the following dimension: 0.5 in. in diameter and 0.19 in. in height.

Fig. 2 shows the layout of the central stripline geometry of circulator #1. The port width has transitions such that the port impedance changes from 50 Ω to Z_{in}. The central metal strips were photoetched through copper foils of thickness 7 mil. Reflection, transmission and isolation coefficients were measured on the devices from 0.05 to 18 GHz utilizing a network analyzer HP8510B. Fig. 3 shows the measured S_{11}, S_{21}, and S_{31} data for circulator #1. Similar results were also obtained for circulators #2 and #3. Table II summarizes the results. We have chosen air to be the dielectric filling material in these devices, since the theory [2] requires the dielectric constant of the filling material to be close to 1, see Table II. From Fig. 3 we see that the stopband of the device extends to more than four times the transmission frequency.

Table II reports on bias magnetic field requirements, transmission frequencies, insertion loss, isolation, and transmission bandwidth as compared to theory. While most of the experimental data compare reasonably well with theory, the transmission bandwidths calculated from S_{21} do show some discrepancy between theory and experiments. When transmission bandwidths are calculated from S_{11} or S_{31}, there is less discrepancy between theory and experiments. As indicated in the theory [2], the transmission through the device is low for frequencies between f_1 and f_2 as defined by

$$f_1 = \gamma H_i, \quad f_2 = \gamma(H_i + 4\pi M_s).$$

In this frequency range μ_{eff} is negative and hence the wave propagation constant k becomes complex. However, experimentally, we find that the transmission coefficients between f_1 and f_2 are relatively high. The transmission bandwidths of the devices calculated from S_{21} are roughly the values predicted by the theory plus the widths of the complex wave-propagation regions given by $f_2 - f_1$. The widths of the complex wave-propagation regions for circulators #1 to #3 are 2.1, 1.4, and 2.8 GHz, respectively. Therefore, we suspect that the approximations imposed in the Green's function calculations pertaining to an asymmetric circulator are inappropriate for frequencies in the range where the wave propagation constants become complex. We also note that these devices exhibit higher insertion loss than expected due to higher value of the linewidths used as well as the impedance mismatch at the input and output ports. The ferrite materials used in fabricating the circulators have linewdiths ΔH about 20 times larger than the value used in the calculations.

Fig. 4 shows the transmission characteristics of a cascade structure involving two identical circulators (circulator #1). The transmission frequency is around 2.0 GHz with 3 dB bandwidth about 3.3 GHz. The insertion loss is 2.1 dB, the isolation is greater than 30 dB, and the stopband extends beyond 18 GHz, which is about 2 octaves of the transmission frequency. The insertion loss of this device can be improved by using ferrites with less magnetic loss and/or better impedance matching network. For example, quarter-wave transformers may be used within the circulator ports to avoid impedance mismatches.

TABLE I
SPECIFICATIONS ON THE FERRITE DISCS FOR CIRCULATORS #1 TO #3

	Type	$4\pi M_s$ (G)	ϵ_f	$\Delta H/4\pi M_s$	h (mm)	D (mm)	N_z
Circ. #1	TT1-414	750	11.3	0.16	1.22	4.4	0.68
Circ. #2	TT2-113	500	9.0	0.30	1.22	7.4	0.79
Circ. #3	TT2-130	1000	12.0	0.32	1.22	3.2	0.60

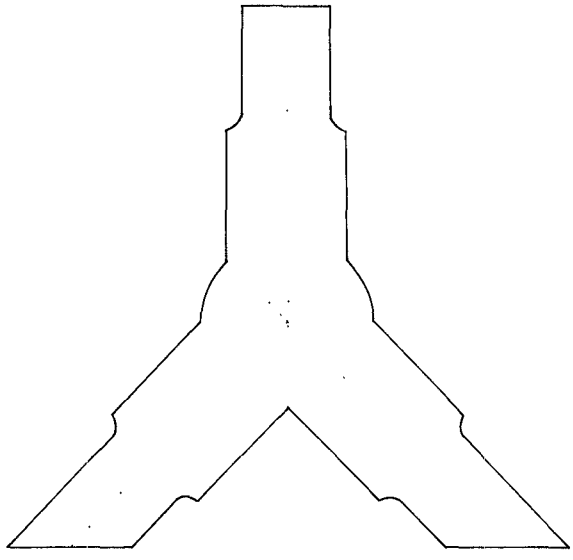

Fig. 2. Layout of the central metal strip of circulator #1.

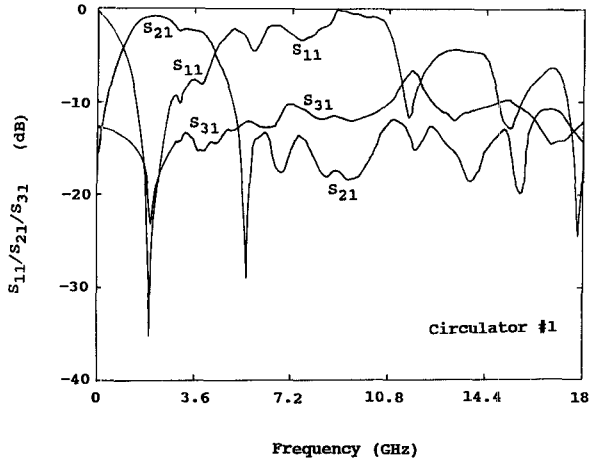

Fig. 3. Reflection, transmission, and isolation data for circulator #1.

TABLE II
THEORETICAL AND EXPERIMENTAL DATA ON ϵ_d, H_o, TRANSMISSION FREQUENCY, INSERTION LOSS, AND BANDWIDTH FOR CIRCULATORS #1 TO #3

		ϵ_d	H_o (KOe)	Tran. Freq. (GHz)	I. L. (dB)	Iso. (dB)	B. W. (GHz)
Circ. #1	Theory	1.04	2.08	1.5	~0.3	≥15	0.6
	Exp.	1.00	1.87	2.0	0.83	~15	3.3
Circ. #2	Theory	0.83	1.45	1.0	~0.3	≥15	0.4
	Exp.	1.00	1.16	2.1	0.82	~16	3.2
Circ. #3	Theory	1.10	2.70	2.0	~0.3	≥15	0.8
	Exp.	1.00	2.26	2.4	0.72	~17	4.4

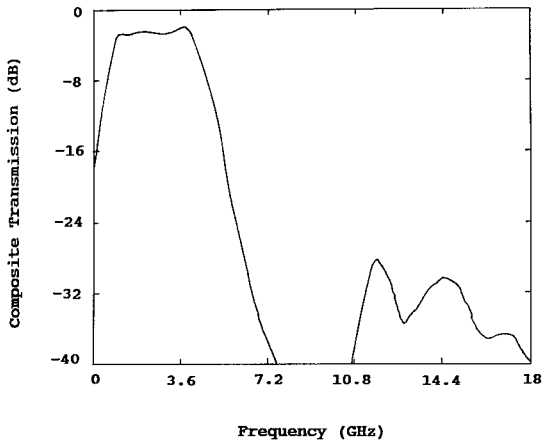

Fig. 4. Transmission data for the cascade structure involving two circulators (circulator #1).

Conclusion

Practical wide stopband filters involving asymmetric stripline Y-junction circulators have been fabricated and tested at microwave frequencies from 0.05 to 18 GHz. The calculated biasing field requirement, transmission frequency, insertion loss, isolation, and stopband frequency range are in reasonable agreement with the corresponding measured values. The ferrite filters were designed to operate away from magnetic resonance so that high power handling capability could be achieved. The fabricated filters show stopbands of 2 octaves and hence can be used extensively as protective elements in a wide frequency range in radome applications. The device's insertion loss can be further improved by using low loss ferrite materials or impedance matching networks to the input and output ports of the device. The passband of the device is wider than theoretically expected. However, the wide transmission band implies increased thermal stability of the device and ease of operation when deployed in a cascade configuration.

References

[1] P. Roeschmann, "YIG filters," *Philips Tech. Rev.*, vol. 32, p. 322, 1971.

[2] H. How, G. Vittoria, and C. Carosella, "Novel filter design incorporating asymmetrical stripline Y-junction circulators," *IEEE Trans. Microwave Theory Tech.*, vol. 39, pp. 40–46, Jan. 1991.

[3] D. K. Linkhart, *Microwave Circulator Design*. Norwood, MA: Artech House, 1989.

[4] L. D. Landau and E. M. Lifshitz, *Electrodynamics of Continuous Media*. New York: Pergamon, 1982, p. 25.

Some Observations on the Design and Performance of Distributed Amplifiers

J. L. B. Walker

***Abstract*—This paper presents closed-form analytic expressions for the voltage and power distribution along the drain line of an ideal distributed amplifier.**

Manuscript received April 23, 1991; revised August 15, 1991.

The author is with Thorn EMI Electronics Limited, Sensors Group, Manor Royal, Crawley, W. Sussex RH10 2PZ England.

IEEE Log Number 9103892.

I. Introduction

A recent paper [1] reports on a computer analysis of a distributed amplifier and shows that a nonuniform power distribution occurs in the drain line, and that over some portions of the frequency band one or more of the active devices may become passive i.e. absorb power rather than generate it. It is the purpose of this paper to present closed-form analytic expressions for the voltage and power distribution along the drain line of an ideal lossless distributed amplifier and to show that the above conclusions are fundamental to its operation.

II. Analysis of an Ideal Distributed Amplifier

An ideal GaAs FET has an equivalent circuit of just a gate-source capacitance C_{gs} at its input, and a voltage-controlled current generator g_m in parallel with a capacitance C_{ds} at its output. Fig. 1 shows an idealized distributed amplifier in which each FET has been replaced by this equivalent circuit. Physically, each gate-source capacitance is symmetrically embedded between a pair of inductors $L_g/2$ and forms a Tee-type constant K filter section [2]. However, the ensuing analysis is simplified if one considers the inductance L_g to be symmetrically embedded between a pair of capacitors $C_{gs}/2$; thus each gate-to-source capacitance C_{gs} in Fig. 1 is represented as two capacitors $C_{gs}/2$ in parallel. Similarly, each drain-to-source capacitance is represented as two capacitors $C_{ds}/2$ in parallel. The Pi type constant K filter section has an image impedance and propagation constant of

$$Z_\pi^g = Z_0^g \Big/ \sqrt{1 - \left(\frac{\omega}{\omega_{cg}}\right)^2} \tag{1}$$

and

$$\theta_g = \cos^{-1}\left(1 - 2\left(\frac{\omega}{\omega_{cg}}\right)^2\right) \tag{2}$$

respectively, where

$$Z_0^g = \sqrt{\frac{L_g}{C_{gs}}} \tag{3}$$

and

$$\omega_{cg} = 2/\sqrt{L_g C_{gs}}. \tag{4}$$

The cascade of constant K filter sections forms an artificial transmission line of characteristic impedance Z_π^g. This transmission line needs to be terminated in source and load impedances of Z_π^g in order that $S_{11} = 0$. If the input and output half-sections are included, then the transmission line needs to be terminated in Z_T^g [2] rather than Z_π^g for $S_{11} = 0$ where

$$Z_T^g = Z_0^g \sqrt{1 - \left(\frac{\omega}{\omega_{cg}}\right)^2}. \tag{5}$$

Assuming, for the moment, that $C_{\text{add}} = 0$ in Fig. 1, then all the preceding equations apply to the drain line also if the subscript or superscript g is replaced everywhere by d.

Now for proper operation of the distributed amplifier one requires [3]

$$\theta_g = \theta_d = \theta \tag{6}$$

and hence, from (2)

$$\omega_{cg} = \omega_{cd} = \omega_c. \tag{7}$$